WPMST1-CPR(18) 20083

P Vondracek et al.

Divertor infrared thermography on COMPASS

Preprint of Paper to be submitted for publication in Proceeding of 30th Symposium on Fusion Technology (SOFT)

This work has been carried out within the framework of the EUROfusion Consortium and has received funding from the Euratom research and training programme 2014-2018 under grant agreement No 633053. The views and opinions expressed herein do not necessarily reflect those of the European Commission.

This document is intended for publication in the open literature. It is made available on the clear understanding that it may not be further circulated and extracts or references may not be published prior to publication of the original when applicable, or without the consent of the Publications Officer, EUROfusion Programme Management Unit, Culham Science Centre, Abingdon, Oxon, OX14 3DB, UK or e-mail Publications.Officer@euro-fusion.org

Enquiries about Copyright and reproduction should be addressed to the Publications Officer, EUROfusion Programme Management Unit, Culham Science Centre, Abingdon, Oxon, OX14 3DB, UK or e-mail Publications.Officer@euro-fusion.org

The contents of this preprint and all other EUROfusion Preprints, Reports and Conference Papers are available to view online free at http://www.euro-fusionscipub.org. This site has full search facilities and e-mail alert options. In the JET specific papers the diagrams contained within the PDFs on this site are hyperlinked

Divertor Infrared Thermography on COMPASS

P. Vondracek[a,b], E. Gauthier[c], M. Grof[d], M. Hron[a], M. Komm[a], R. Panek[a], the EUROfusion MST1 team[e]

[a] *Institute of Plasma Physics of the CAS, Prague, Czech Republic*
[b] *Faculty of Mathematics and Physics, Charles University, Prague, Czech Republic*
[c] *CEA/DSM/IRFM, CEA Cadarache, Saint-Paul-les-Durance, France*
[d] *Faculty of Nuclear Sciences and Physical Engineering, Czech Technical University in Prague, Prague, Czech Republic*
[e] *See the author list of Meyer H. et al 2017 Nucl. Fusion 57 102014*

Abstract

A new fast divertor infra-red thermography system was put into operation on COMPASS. It provides full radial coverage of the bottom open divertor with pixel resolution ~ 0.6–1.1 mm/px on the target surface and time resolution better than 20 µs. Individual parts of the system are described: a fast IR camera TELOPS Fast-IR 2K, its magnetic shielding box and a positionable holder, a 1m long IR endoscope consisting of 14 Ge and Si lenses securing off-axis view from an upper inner vertical port. A special graphite divertor tile optimized for IR thermography is presented as well. It is equipped with a heating system allowing tile preheating up to 250 °C, embedded thermoresistors, a calibration target (a deep narrow hole acting as a black body radiator) for in-situ system calibration including estimation of the target surface emissivity and a roof-top shaped structure increasing magnetic field incidence angles above 3 degrees.

Laboratory tests of the system performed during its commissioning are presented. The global transmission of the optical system was found to be $\tau \approx 40\,\%$. Poor spatial resolution compared to the design value was observed and will require additional optimization of the system.

First experimental results are presented: divertor heat flux profiles in L-mode with the heat flux decay length $\lambda_q^{\mathrm{omp}} = 2.3$–$3.1$ mm and average H-mode heat flux profiles in an inter-ELM period and during an ELM heat flux maximum $\lambda_q^{\mathrm{omp}} \approx 0.6$ mm and $\lambda_q^{\mathrm{omp}} \approx 6.7$ mm, respectively.

Keywords: Infra-red thermography, scrape-off layer, tokamak

1. Introduction

The COMPASS tokamak [1] is equipped with an open lower graphite divertor. Direct observation of approx. 190×152 mm^2 of the divertor region from the top of the machine is secured by the divertor infra-red (IR) system, which was commissioned in 2018. This system provides measurements of the full radial profile of the divertor surface temperature with pixel size ~0.6–1.1 mm/px on the target surface,~0.04–0.12 mm/px mapped to the outer midplane (OMP), frame rate up to 57 kHz (320×4 px) and up to 90 kHz with a limited radial divertor coverage (64×4 px). See Figure 8 in [2] for an overview of the field of view (FOV) of the system.

2. IR system overview

The IR system consists of Telops FAST-IR 2K IR camera sensitive to wavelength range 3–5.5 µm, ~1 m long IR endoscope, sapphire vacuum window and a special graphite divertor tile optimized for IR thermography. Furthermore the IR camera is placed inside a magnetic shielding box made of 8 mm thick soft iron with embedded water cooling. The IR camera is mounted to the main tokamak support structure via a massive holder enabling precise positioning of the camera (radial and toroidal movement and tilting with the pivot point near the vacuum viewport). The magnetic shielding bow is supported by a separate holder in order to minimize transfer of vibrations to the camera. The system overview is shown in Figure 1.

The IR camera is connected via a Camera Link interface to a MATROX frame grabber placed on a PCI Express bus of a dedicated high performance personal computer. A PCI Express SSD disk is used to store camera data with very high data throughput.

The IR endoscope contains 4 Germanium and 10 Silicon lenses and is divided into two separated parts. First part consists of two subassemblies (lenses L1-L3 and L4-L11) decentred mutually by 2.1 mm providing radial outward shift of the FOV as the endoscope is placed above the inner edge of the divertor. The second part is triplet L12-L14 mounted directly to the camera body and secures focusing of the system. All the optical surfaces including the sapphire window are treated with an antireflective IR coating decreasing surface reflections below 2 % at a single surface.

The special divertor tile in the field of view of the IR system is precisely aligned with neighboring tiles in order to secure elimination of magnetic shadowing and proper inclination compared to magnetic field necessary for extraction of the parallel heat flux. An embedded heating cable at the bottom tile surface in combination with embedded Pt100 thermistor and

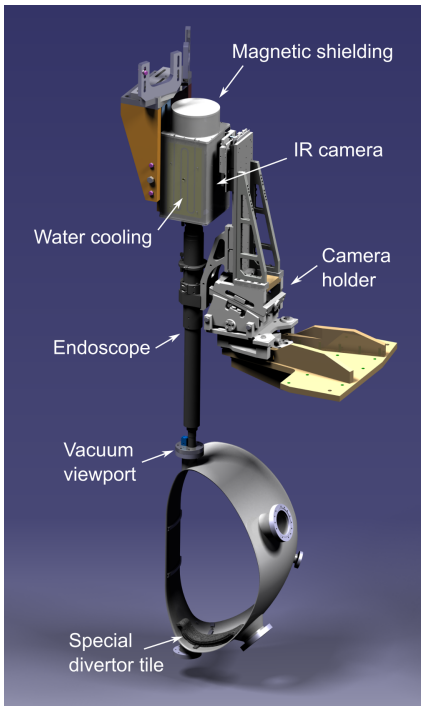

Figure 1: An overview of the divertor IR system on COMPASS.

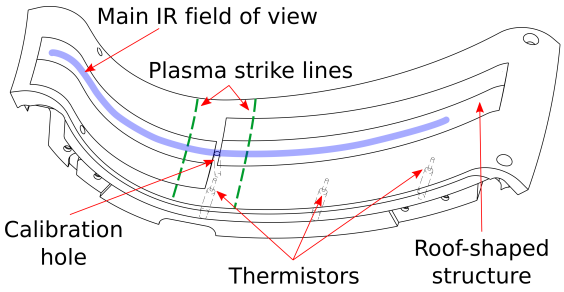

Figure 2: The special graphite divertor tile optimized for IR thermography. Typical IR FOV is marked in blue, typical strike lines positions are shown by the green dashed lines.

a narrow deep hole ($3 \times 15\,\mathrm{mm}^2$) in the top surface acting as a black body radiator enable in-situ calibration of the tile surface emissivity and measurements with increased tile base temperature (up to ~250 °C). Signal from another two thermistors is acquired several seconds before, during and after a plasma discharge providing reference temperature for validation of IR data. Heating of the tile is interrupted in the same time, so that the tile temperature can equalize before the discharge and in order to minimize electromagnetic forces acting on heating wires in presence of tokamak magnetic field because of $\mathbf{E} \times \mathbf{B}$ forces. A 1 mm high roof-shaped structure on the top surface increases magnetic field lines incidence angles (roof inclination 3°) to secure precise extraction of the parallel heat flux and to increase detector signal. The tile design is visualized in Figure 2. An example of time evolution of the tile surface emissivity during an experimental campaign is shown in Figure 3.

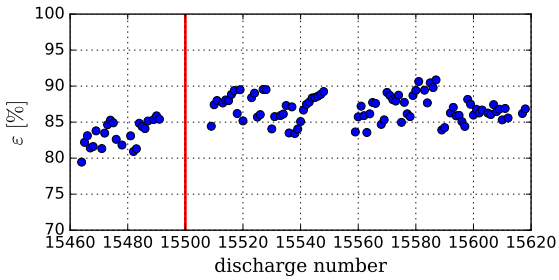

Figure 3: Time evolution of the surface emissivity of the special graphite divertor tile. The red line indicates a boronization of the vacuum vessel.

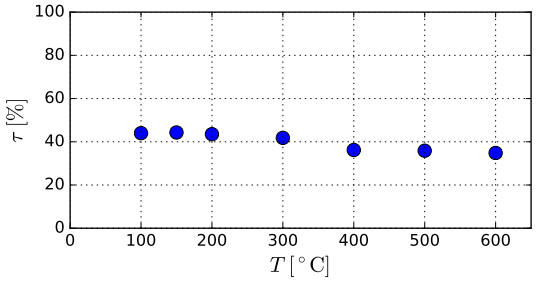

Figure 4: The global transmission of the IR endoscope and sapphire window for radiation of a black body with different temperature.

3. Optical performance

The optical performance of the IR endoscope was tested in laboratory during the commissioning of the system. The global transmission of the endoscope combined with the sapphire vacuum window was measured using a calibration black body source in the range 100–600 °C. The average transmission $\tau \approx 40\,\%$ was found—see Figure 4.

The spatial resolution of the system was tested using the slit experiment as described in [3]. High resolution profile across a 1 mm wide slit placed 720 mm from the sapphire window was obtained by moving the slit laterally with a step 50 µm. 1 px corresponds to ~ 0.6 mm in the object plane. The profile (image) is visualized by the red dots in Figure 5, the corresponding view of the slit by an ideal camera (object) has a form of a *door function* and is shown by the green line. The camera image is a convolution of the object with the *point spread function* (PSF)

$$\text{Image} = \text{Object} * \text{PSF}. \tag{1}$$

A ratio of Fourier transforms of the image and object was calculated in order to get the Fourier transform of the camera PSF, the so-called *optical transfer function* (OTF). The modulus (magnitude) of the OTF, the *modulation transfer function* (MTF), was then multiplied by the *sampling MTF* to take into account a random position of an object with respect to the detector [3]. The resulting *total MTF* was fitted by a Gaussian function in frequency space—see Figure 6. The standard deviation σ of the corresponding Gaussian function in spatial space was used to characterize the spatial resolution of the system. A profile of σ across the FOV is shown in Figure 7. Strong variation of $\sigma \approx 0.6$–0.95 mm (1–1.6 px) was found, which is much larger

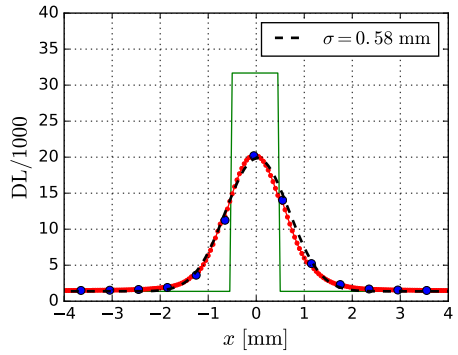

Figure 5: Signal of an ideal camera viewing 1 mm wide slit (green) and corresponding signal from the tested IR system (blue). The red dots were obtained by moving the slit with 50 µm step. The dashed line is a synthetic reconstruction of the IR system view based on measured spatial resolution (see Figure 6).

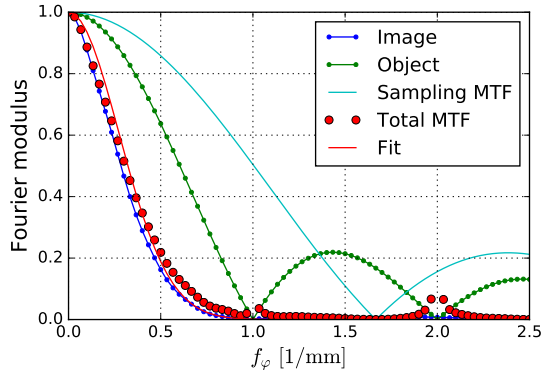

Figure 6: Normalized Fourier modulus of the measured slit profile (image, blue) and of the perfect object (green). The sampling MTF is shown in cyan, the resulting total MTF by the red dots and its fit by the Gaussian function by the red line. σ = 0.58 mm in spatial space for this case.

than the expected value and further optimization of the system is therefore foreseen.

4. Experimental results

4.1. L-mode

Several L-mode divertor heat flux profiles were acquired during system commissioning. Overview of main plasma parameters of used discharges is shown in Figure 8 (#16882: I_p = 180 kA, B_tor = 1.15 T, n_e = 4×10^{19} m^{-3}, #16972: I_p = 240 kA, B_tor = 1.15 T, n_e = 2.5×10^{19} m^{-3}, #17002: I_p = 210 kA, B_tor = 1.38 T, n_e = 4×10^{19} m^{-3}).

The THEODOR code [4] was used to calculate the heat flux from the measured time evolution of the divertor temperature. Obtained heat flux profiles were fitted by convolution of an exponential function (with the characteristic decay length λ_q) and a Gaussian function (with standard deviation S) as described in [5]. Profiles mapped to the outer midplane are shown in Figure 9. The plasma current scan shows expected behavior of an increasing parallel heat flux at separatrix, $q_{\parallel,0}$, and a decreasing heat flux decay length, λ_q, with increasing plasma current, I_p.

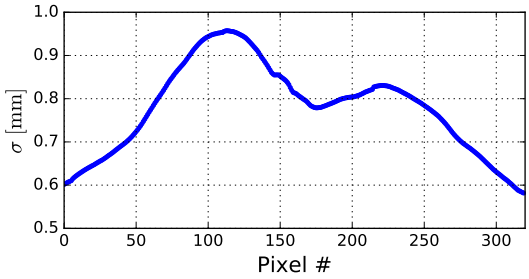

Figure 7: Dependence of the standard deviation σ of the total MTF of the divertor IR system as a function of the radial position in the FOV (in the center of the FOV in the toroidal direction).

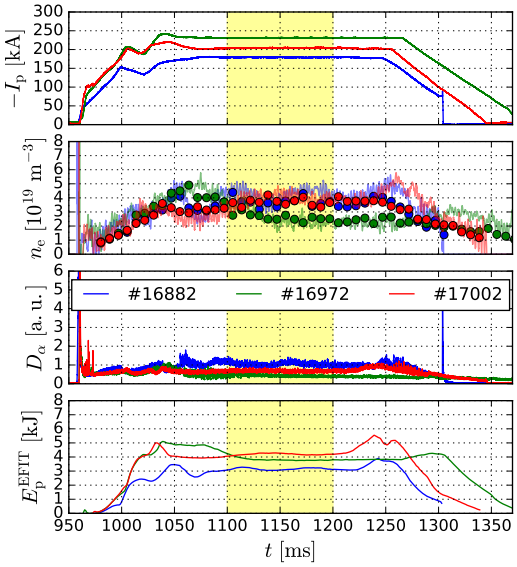

Figure 8: An overview of parameters of discharges used for the L-mode divertor heat flux analysis. From top to bottom: plasma current, line averaged electron density as measured by the interferometer (solid lines) and the Thomson scattering (dots), D_α line signal, plasma stored energy calculated by the EFIT code. Analyzed profiles are time averaged over the highlighted interval.

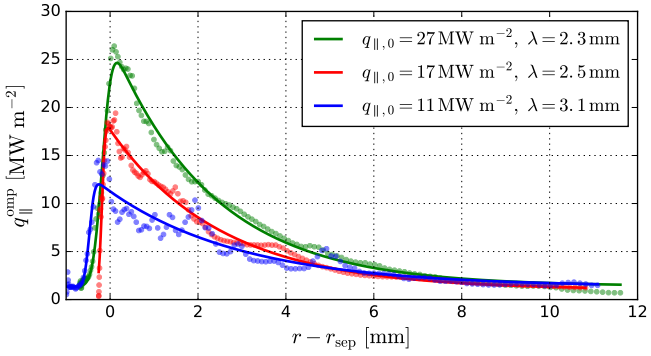

Figure 9: Outer divertor heat flux profiles measured using the new divertor IR system for L-mode discharges #16882 (blue), #16972 (green) and #17002 (red). Profiles are mapped to the OMP.

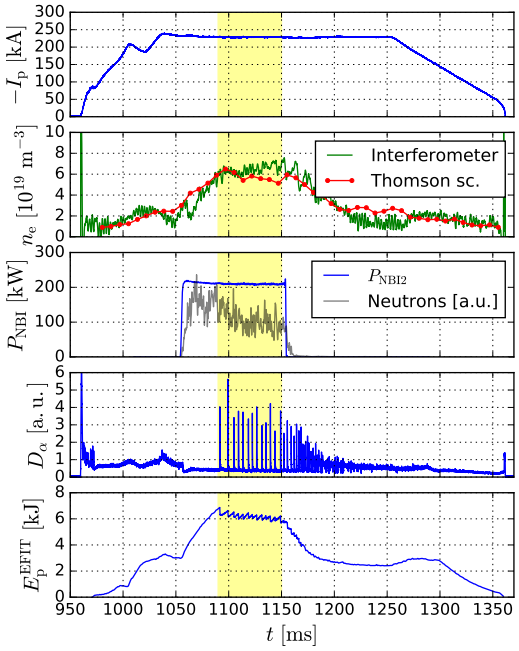

Figure 10: Parameters overview of the discharge #16908 used for the H-mode divertor heat flux profiles analysis. From top to bottom: plasma current, line averaged electron density, injected NBI power and signal from neutron detectors, D_α line signal, plasma stored energy calculated by the EFIT code. Analysed profiles are time averaged over the highlighted interval.

4.2. H-mode

Outer divertor heat flux profiles from neutral beam injection (NBI) heated H-mode discharge #16908 are analyzed in this section. Overview of main plasma parameters of the used discharge is shown in Figure 10 (I_p = 230 kA, B_{tor} = 1.15 T, $n_e = 6 \times 10^{19}$ m^{-3}, P_{NBI} = 210 kW).

In H-mode, surface effects (mainly presence of dust particles forming micro hot spots) strongly influence heat flux calculation of fast transients like edge localised modes (ELMs). The heat transmission coefficient α is implemented in THEDOR for compensation of these effects. α was set individually for each pixel in order to get zero heat flux after the plasma discharge in t = 1370 ms.

An average inter-ELM heat flux profile was calculated by averaging heat flux derived in 200 µs long inter-ELM periods preceding to 13 ELMs in the time interval t = 1090–1150 ms. Similarly, average heat flux profile during ELM heat flux maximum was calculated for the same set of ELMs. The spatially averaged heat flux across the whole divertor was used for detection of ELM timing. Comparison of both profiles is shown in Figure 11 for the outer divertor region (all mapped to the OMP). Very narrow inter-ELM heat flux profile with $\lambda_q^{omp} \approx 0.6$ mm is observed. Heat flux profile broadening by factor ~11 is observed when comparing the inter-ELM and the ELM heat flux maximum profiles.

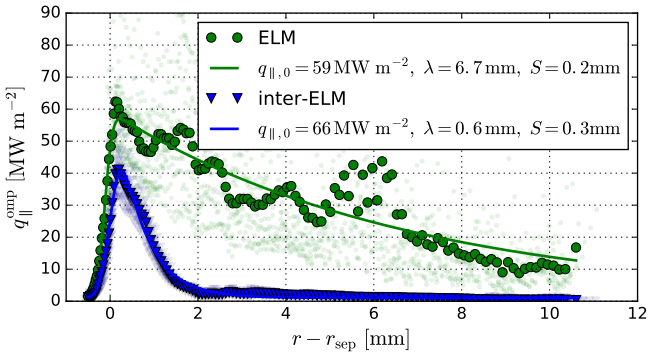

Figure 11: Radial outer divertor heat flux profile mapped to the OMP for inter-ELM (blue) and during ELM heat flux maximum (green) for the discharge #16908. Small dots are data for individual ELMs, large dots are average values for the set of 13 ELMs in t = 1090–1150 ms.

5. Conclusion

A new divertor IR system was put into operation on the COMPASS tokamak. It provides routine fast measurement of time evolution of the divertor temperature distribution and consequently of the radial profile of the heat flux for both the inner and the outer divertor target. Global transmission of optical part of the system $\tau \approx 40$ % was found during its commissioning. Non-optimal spatial resolution of the system will require additional inspection and optimisation of its optics to reach design values, nevertheless the performance is sufficient for basic heat flux profile measurements.

First experimental divertor heat flux measurements using the new system were successfully performed in both L-mode and H-mode, proving that the system can provide unique results with exceptional temporal resolution and with coverage of both the inner and the outer divertor regions.

Acknowledgments

This work was co-funded by MEYS projects number 8D15001 and LM2015045 and by Czech Science Foundation project GA15-10723S. This work has been carried out within the framework of the EUROfusion Consortium and has received funding from the Euratom research and training programme 2014-2018 under grant agreement No 633053. The views and opinions expressed herein do not necessarily reflect those of the European Commission.

References

[1] R. Panek, et al., Status of the compass tokamak and characterization of the first H-mode, Plasma Physics and Controlled Fusion 58 (2016) 014015.
[2] P. Vondracek, et al., Fast infrared thermography on the COMPASS tokamak, Fusion Engineering and Design (2017).
[3] Y. Corre, et al., Methodology for heat flux investigation on leading edges using infrared thermography, Nuclear Fusion 57 (2017) 016009.
[4] A. Herrmann, et al., Energy flux to the ASDEX-Upgrade diverter plates determined by thermography and calorimetry, Plasma Physics and Controlled Fusion 37 (1995) 17.

[5] T. Eich, et al. (ASDEX Upgrade Team), Inter-ELM power decay length for JET and ASDEX Upgrade: Measurement and comparison with heuristic drift-based model, Phys. Rev. Lett. 107 (2011) 215001.